Available online at www.sciencedirect.com

ScienceDirect

journal homepage: www.elsevier.com/locate/he

Polyaniline and polyaniline-carbon black nanostructures as electrochemical capacitor electrode materials

Marcela A. Bavio [a,b,*], Gerardo G. Acosta [a,b], Teresita Kessler [a,c]

[a] Facultad de Ingeniería, INTELYMEC-CIFICEN, UNCPBA, Avda. del Valle 5737, Olavarría, Buenos Aires, Argentina
[b] CONICET, Av. Rivadavia 1917, C1033AAJ Buenos Aires, Argentina
[c] CICPBA, Calle 526 entre 10 y 11, 1900 La Plata, Argentina

ARTICLE INFO

Article history:
Received 21 October 2013
Received in revised form
9 December 2013
Accepted 3 January 2014
Available online 30 January 2014

Keywords:
Polyaniline nanotubes
Carbon black
Nanocomposites
Supercapacitors

ABSTRACT

Polyaniline (PANI) and polyaniline-carbon black (PANI-CB) nanostructures were developed and their behavior in relation to supercapacitors properties was tested. Different nanostructures were prepared by a simple chemical method of self-organization. SEM and TEM images revealed PANI nanotubes of ca. 95 nm in diameter; nanoparticles, nanobelts, nanosheets and/or nanotubes could be recognized in PANI-CB nanocomposites as a result of the use of CB particles with and without chemical pretreatment, CBf and CBnf, respectively. From EDS, XRD, UV–Vis and FTIR characterization techniques, the development of the various nanostructures was attributed to the chemical polymerization process that provoked a doped PANI state and hydrogen links that stabilized the changes in the structures. The resulted morphologies influenced the capacitance, specific power and specific energy values. PANI-CBf nanocomposites displayed improved capacitive properties in H_2SO_4 solutions, namely 1486 F g^{-1} at 2 A g^{-1}. The charge–discharge tests indicated that the loss of capacitance during the charge/discharge cycles was lower than 18% for the checked materials.

1. Introduction

Energy consumption/production that relies on the combustion of fossil fuels is having a severe worldwide impact on economics and ecology. The electrochemical energy production is under consideration as an alternative energy/power source, as long as this energy consumption is designed to be more sustainable and environmentally friendly. Operative systems for electrochemical energy storage and conversion include batteries, fuel cells, and electrochemical capacitors or supercapacitors [1]. The electrochemical capacitors differ from the conventional dielectric capacitors in their special energy storage mode. These systems store electrical energy through double-layer charging steps, faradaic processes or a combination of both ways. The main interest of these devices is their capability to deliver high specific peak power, associated with a good specific energy [2,3]. The process is completely reversible and the charge-discharge cycles can be repeated over and over again, virtually without limit.

The electrochemical capacitors are robust devices that can improve the effectiveness of battery-based systems by decreasing the number of required batteries and by reducing the frequency of their replacement. The carbon family offers a

* *Corresponding author*. Facultad de Ingeniería, INTELYMEC-CIFICEN, UNCPBA, Avda. del Valle 5737, Olavarría, Buenos Aires, Argentina.
E-mail addresses: mbavio@fio.unicen.edu.ar, marchu_b@yahoo.com (M.A. Bavio).
0360-3199/$ – see front matter
http://dx.doi.org/10.1016/j.ijhydene.2014.01.018

number of components to be applied as electrode supercapacitors materials; they are, among others, activated carbon, carbon black (CB), carbon nanotubes (CNT) and graphene [4–6]. In particular, CB is considered as a promising material due to its particular ordered nanostructure, low density, large surface area, high thermal stability, good electrical conductivity, lower cost, corrosion resistance, less material requirement for percolation, and ease of processing into host polymers [7–9].

A route to enhance the capacitance of a material is synthetizing composites through the proper combination of substances, among others ruthenium oxide and conductive polymers [6,10,11].

Polyaniline (PANI) is one of the most extensively studied conducting polymers, because it can be obtained through not expensive ways, it is stable at room temperature and is an ionic-electronic conductor in a wide potential range [12–14]. There are different chemical and electrochemical methods of synthesis producing easily a large amount of substance or obtaining high purity polymer samples, respectively. The polymeric nanostructures present unique characteristics derived from their nanoscale size; among others, high electrical conductivity, large specific surface, a mixed ionic-electronic conductivity mechanism and a high discharge capacity to mass ratio. Methods of hard and soft templates are used to obtain conducting polymer nanostructures, being the microemulsions technique the most promising route [15].

Conducting polymers and carbon materials can be combined properly forming composite materials with properties that can be used adequately in practical systems [16–19].

This paper reports the synthesis by in-situ oxidative polymerization of polyaniline nanotubes and polyaniline - carbon black nanocomposites, and their behavior related to supercapacitors properties are scrutinized. The initial synthesis mixture consists in an acid solution of aniline with a surfactant agent, without additions and with the incorporation of carbon black particles (Vulcan XC-72R), both as-received and pretreated ones. The structure and morphology of the obtained nanostructures were analyzed by SEM, TEM, EDS, RDX, FTIR and UV–Vis. The electrochemical capacitance performances of the developed and characterized nanostructures were investigated in acid solution showing an outstanding behavior.

2. Experimental

2.1. Synthesis of nanostructures of PANI and PANI-CB

The synthesis solution was prepared mixing 0.045 g of aniline, 0.30 mL of 0.25 M HCl and 0.005 g of sodium dodecyl sulfate (SDS) in 18 mL of distilled water under constant magnetic stirring, at room temperature (25 °C) for 20 min. Then, 2 mL of 0.24 M ammonium persulfate (APS) were added to the initial mixture and the resulting dispersion was stirred vigorously for half a minute. Afterwards, it was left for 24 h at 25 °C without agitation to progress with the polymerization. A residue is obtained after filtering and washing repeatedly the obtained precipitate. Finally, it was dried for 24 h at 60 °C.

PANI-CB nanostructures were synthetized applying the procedure just described, but with the addition of 0.1 mg mL^{-1} of CB particles to the initial aqueous dispersion. Carbon black (Vulcan XC-72R) was used either as received (CBnf) or pretreated (CBf) ones.

The applied pre-treatment consisted in adding CB particles to 2.2 M nitric acid at room temperature. After stirring the preparation with an ultrasonic bath, it was kept at room temperature for 20 h, then filtered and washed to achieve neutral pH in the filtrate solution. Finally, the residue consisting in CBf particles was dried at 37 °C for 2 h [20].

2.2. Characterization methods

The synthetized nanostructures were characterized through various physicochemical techniques. Energy diffraction spectroscopy (EDS) and Scanning Electron Microscopy (SEM) were performed with an EDAX Genesis XM4 – Sys 60 analyzer coupled to scanning electron microscope Jeol JSM-6460LV; and the Transmission Electron Microscopy (TEM) micrographs with a JEOL model 100CX operated at 100 KV. The TEM images were processed with Image J to determine the particle size.

FTIR spectra were recorded between 4000 and 400 cm^{-1} using a Nicolet, Magna 500 (250–4000 cm^{-1}) equipment with CsI optics.

UV–Vis spectra were obtained for the different samples in aqueous solution, using a spectrophotometer UV-1800 PC MAPADA in the 250–900 nm range.

The X-ray diffraction (XRD) patterns of samples were recorded using an X-ray diffractometer (Philips PW 3710) and Cu Kα line ($\lambda = 1.5451$ nm) with cooper anode.

2.3. Preparation of electrodes and electrochemical measurements

The working electrodes were assembled through the following routine. Firstly, PANI or PANI-CB nanostructures were dispersed in pure isopropanol and a suitable amount of Nafion solution was added in order not to exceed 5%. The dispersion was stirred using an ultrasonic bath for 5 min. Finally, the suspension was settled on a mirror-polished glassy-carbon electrode using a micropipette, being the amount of PANI or PANI-CB nanostructures of 0.2 mg cm^{-2}.

Typical electrochemical techniques such as cyclic voltammetry and galvanostatic charge/discharge measurements were used to study the capacitive behavior of the synthetized materials. Runs were carried out in the 0.0–1.0 V (vs. RHE) voltage range in 0.5 M H_2SO_4. I/V profiles were registered varying the scan rates from 10 to 100 mV s^{-1}. The charge/discharge curves were recorded at various current density values in the 2–100 A g^{-1} range.

All electrochemical experiments were performed in a three-electrode cell thermostatized at 25 °C, using a large Pt sheet and a Ag/AgCl (sat.) electrode as counter and reference electrodes, respectively. The connected potentiostat/galvanostat was EG&G PAR Model 362.

3. Results and discussion

3.1. SEM and TEM characterization

Fig. 1 shows SEM and TEM micrographs of different PANI and PANI-CB nanostructures. PANI nanotubes of ca. 15 μm length

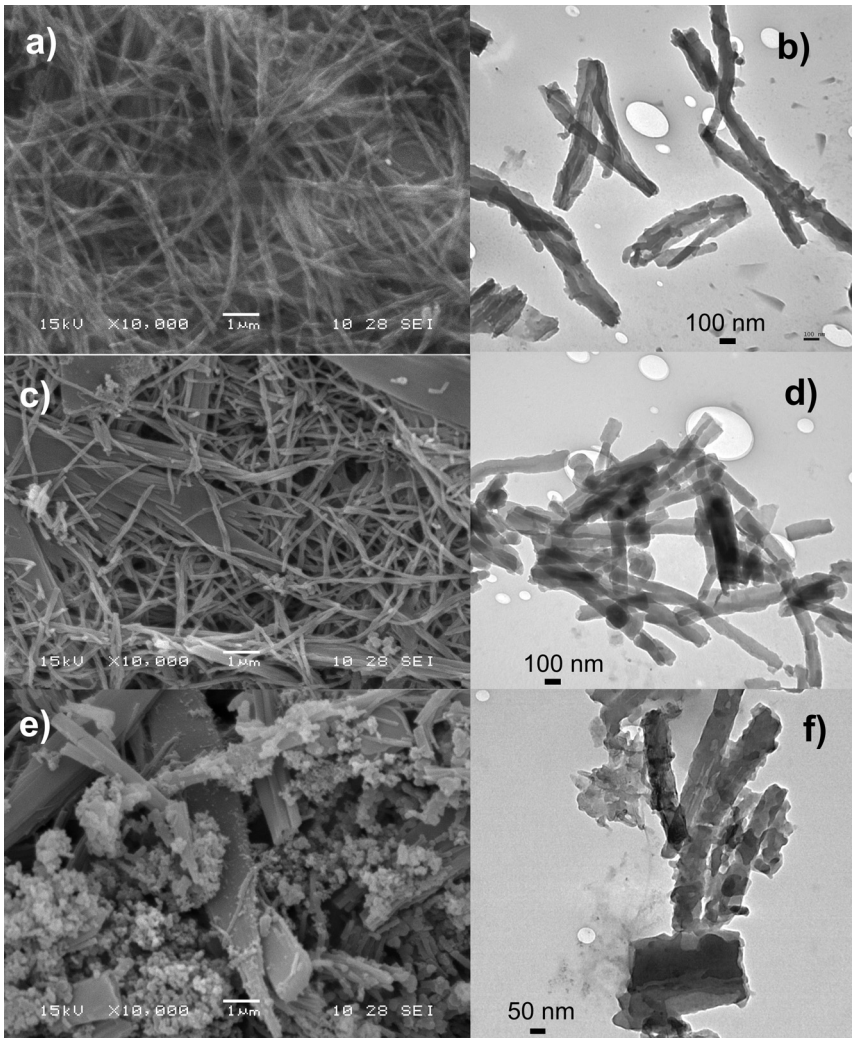

Fig. 1 – SEM and TEM images of a–b) PANI, c–d) PANI-CBf and e–f) PANI-CBnf nanostructures.

and an outer diameter of 95 nm (Fig. 1a and b) are obtained when synthetizing aniline solution without additions. The incorporation of CB particles to the initial solution promotes the formation of different morphologies, depending on the added CB.

The addition of CBf particles promotes the development of nanostructures with different shapes such as nanobelts and nanotubes (Fig. 1c and d). PANI-CBf nanobelts have a thickness of ca. 100 nm, a wide of 2 μm and 12–15 μm in length. PANI-CBf nanotubes have a mean outside diameter of ca. 95 nm and 15 μm in length. On the other hand, when adding CBnf particles, the development of various nanostructures is evident: nanotubes (diameter: 95 nm, length: 5–8 microns), nanoparticles (diameter: 85–90 nm) nanobelts (length: 10-12 microns, width: 1 micron and thickness: 100 nm) and nanosheets (length: 0.5 microns, width: 0.3 microns and thickness: 95–100 nm) (Fig. 1e and f).

According to other researchers [21,22], the type of nanostructures is determined by variables such as the concentration ratio between aniline and APS ([aniline]/[APS]), the acid and dispersant concentrations in the reaction mixture, and the temperature. Common synthesis process starts at a pH of ~ 7.5 and in 24 h the pH drops to ~1.0 and different nanostructures are formed as a function of pH, from nanoflakes to fibrillar nanostructures [22].

When adding CBf, the structure of the developed PANI composites adopts nanobelts and nanotubes morphologies. To sustain this fact, it must be taken into account that in the PANI synthesis mechanism, anilinium cations are formed in the first step of the polymerization process [15]. The oxidizing chemical pretreatment done to the CB particles provokes the formation of carboxyl, hydroxyl and carbonyl surface groups [23]. Thus, when adding CBf to the polymerization mixture, the negatively charged functional groups of the CBf interact with the anilinium cations, favoring the adsorption of the CBf and promoting the growth of polymer chains from them. The same type of interaction was reported when using oxidized carbon black and graphene oxide for the synthesis of various polyaniline nanocomposites [18–24].

In the case of adding CBnf, the synthesized product is not morphologically homogeneous. It has been pointed out that the formation of self-assembled PANI nanotubes depends on

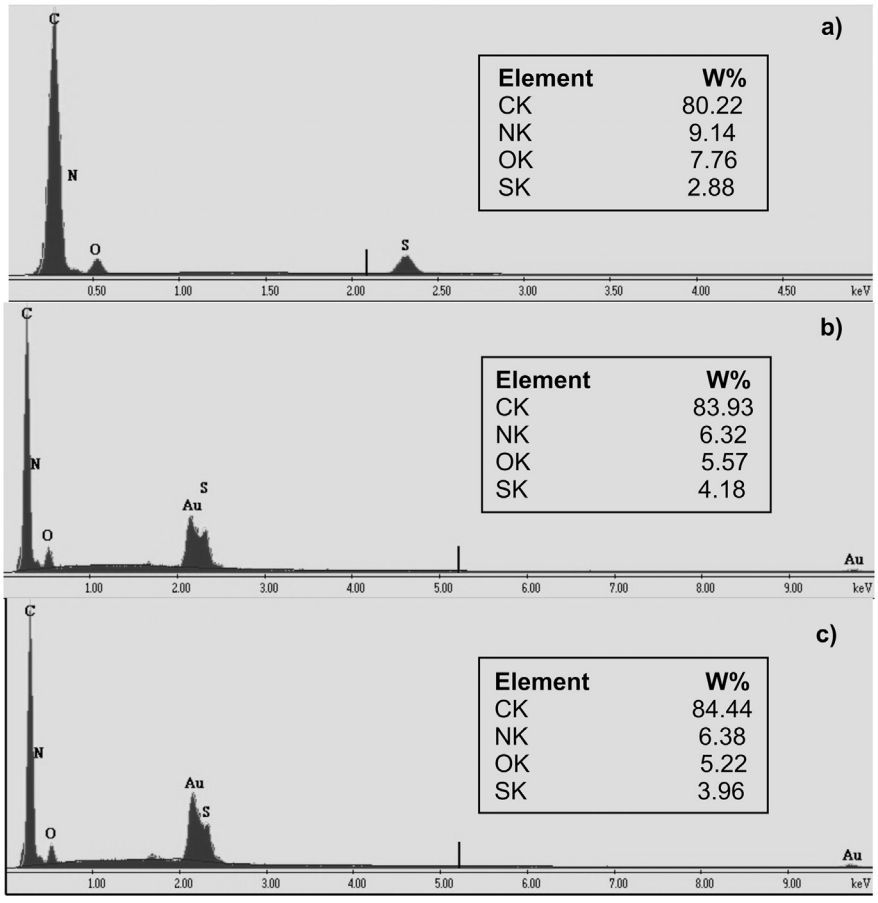

Fig. 2 – EDS spectra of a) PANI, b) PANI-CBf and c) PANI-CBnf nanostructures.

molecular interactions such as hydrogen bondings, van der Waals forces and π-π stacking [22]. A two-step mechanism has been proposed for the formation of nanofibers or nanotubes. The first step comprises the formation of nanosheets in the first stage of the oxidative polymerization process, at higher pH. These nanosheets tend to decrease their surface energy by two ways. Through stacking, relatively thick (~30–100 nm) nanoflakes are built and by rolling or curling, oligomeric nanotubes are developed. The second step occurs at lower pH when polyaniline polymerizes either on the oligomeric nanotube walls making their walls thicker or as grains on the walls of the smooth nanotubes, giving the final form of the nanotubes or nanorods [22].

3.2. *Energy dispersive spectroscopy X-ray (EDS)*

Fig. 2 shows the EDS spectra of synthetized nanomaterials, stating the presence of C, N and O. It was found a significant amount of S, indicating a doped PANI structure as a result of using APS and SDS during the synthesis [25]. The S percentage is higher in PANI-CBf and PANI-CBnf nanocomposites.

3.3. *X-ray diffraction*

Fig. 3 shows the X-ray diffraction patterns of the PANI and PANI-CB nanocomposites. The main diffraction peaks are at 2θ values of 12.2°, 15.2°, 18.4°, 22.4°, 24.6°, 28.3° and 29.2°. These peaks are characteristic of polyaniline in its doped emeraldine salt form. The peaks are superimposed on a broad background, which suggests the presence of an amorphous phase. The peaks at 18.4° and 24.6° are usually assigned to the periodicity parallel and perpendicular to the polymer chain,

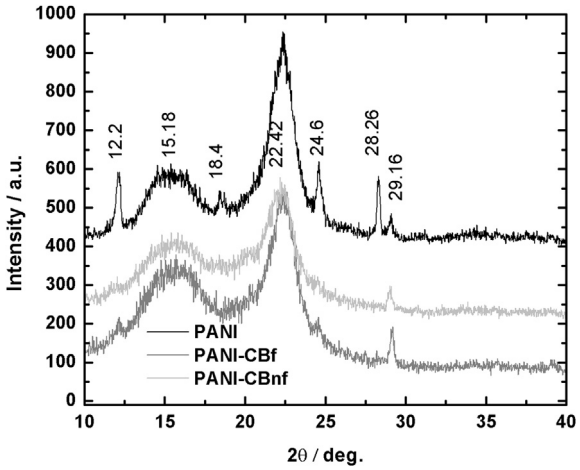

Fig. 3 – XRD patterns of PANI, PANI-CBf and PANI-CBnf nanostructures.

respectively. The peaks at 22.4° and 28.3° (corresponding to spacing of 3.1 and 3.8Å) could be due to a periodicity caused by π-π stacking of rigid phenazine-like structures [22,26].

3.4. FTIR spectra

In Fig. 4, FTIR spectra are presented showing several bands that appear in all the PANI nanostructures spectra [21,25]. The position of the common bands and the corresponding assignment are stated as follows: 1142 cm^{-1} (assigned as –N=quinoid=N–), 1305 cm^{-1} (CN stretching with aromatic conjugation), 1498 and 1585 cm^{-1} (C=C stretching in benzoides and quinoid rings respectively), 2847 and 2916 cm^{-1} (CH stretching of $-CH_3$ and $-CH_2-$, respectively, which shows the presence of SDS in the synthesized products). As reported by Zhou [21], the anionic surfactant added in the polymerization solution contributes doping the PANI chain establishing electrostatic interactions with the anilinium cation at the beginning of the reaction and then, building a supramolecular structure [25].

In the nanostructures spectra, a distinguishable band is present at 1042 cm^{-1}; it is attributed to the substitution of S=O groups in the 1,2,4-aromatic rings, indicating a doped PANI structure as a result of using APS during the synthesis. These results agree with the EDS results, where the presence of S was determined. Another band located at 3250 cm^{-1} is assigned to NH-stretching associated to different of intra- and inter-molecular hydrogen bonds in secondary amines. In the presence of a sulfonate group, a hydrogen bond such as the NH ... O type can be proposed. The presence of hydrogen bonds is indicative of a self-organization process of PANI chains in supramolecular assemblies and can be associated to the stabilization of the nanotubes [21,25]. These results are consistent with those found in the analysis by UV–Vis spectroscopy, confirming the presence of groups that tend to form hydrogen bonds.

Furthermore, other bands must be indicated as contributions to the final formation of the nanostructures, including the ones located at 825 cm^{-1} (CH deformation out of plane in benzoides rings), at 692 cm^{-1} (CC out of plane deformation of rings monosubstituted aromatic), at 1242 cm^{-1} (CN–stretching of secondary aromatic amines) and at 1446 cm^{-1} (presence of branched structures such as phenazine) [22,24].

3.5. UV–Vis spectra

UV–Vis spectra of PANI nanotubes and PANI-CB nanocomposites are shown in Fig. 5. PANI and PANI-CB nanostructures present two adsorption zones. One of these bands is located in the 300–450 nm region (possibly overlapping), related to PANI chain protonation. The other band between 600 and 850 nm is attributed to the π-polaron transition [26,27,21].

The nanostructures spectra has three peaks at 300, 360 and 440 nm, which is due to the superposition of bands corresponding to the π-π* transition of para-substituted benzoides segments and a weak adsorption n-π*. This is consistent with the presence of substituted quinone (strong π-π* peak centered at 250–314 nm, a medium π-π* peak centered at 308–398 nm, and in some cases, a weak n-π* band centered at 424–525 nm) and oligomer-type structures superimposed leucoemeraldine [22]. Substituted quinones are present in hydrolytic reactions at high pH in the presence of a strong oxidizing agent and it is attributed to polyaniline chain protonation.

Moreover, the emeraldine base form of polyaniline usually absorbs strongly in two areas, with maxima at 320–330 and 600–660 nm. The first band is assigned to π-π* excitation of the para-substituted benzenoid segment (–B–NH–B–NH), whereas the other is associated with the excitation of the quinoid segment (–N=Q=N–) [27].

3.6. Cyclic voltammetric studies

Voltamperommetric runs of the prepared nanostructures are carried out between 0.0 V and 1.0 V at various scan rates in order to evaluate their electrochemical characteristics. The typical voltammograms of the nanocomposites are shown in Fig. 6. The anodic and cathodic current peaks assigned to PANI leucoemeraldine/emeraldine pair at ca. 0.4 V are clearly distinguished [13]. At all scan rates, pronounced reversible redox waves are observed in the profiles of PANI-CBf and PANI-CBnf nanocomposite electrodes, indicating their better

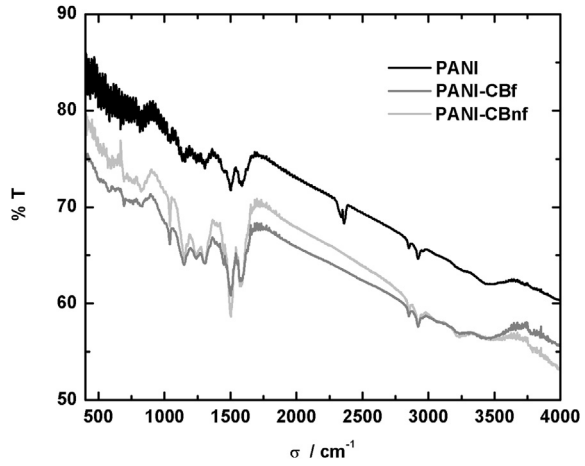

Fig. 4 – FTIR spectra of the synthetized nanostructures.

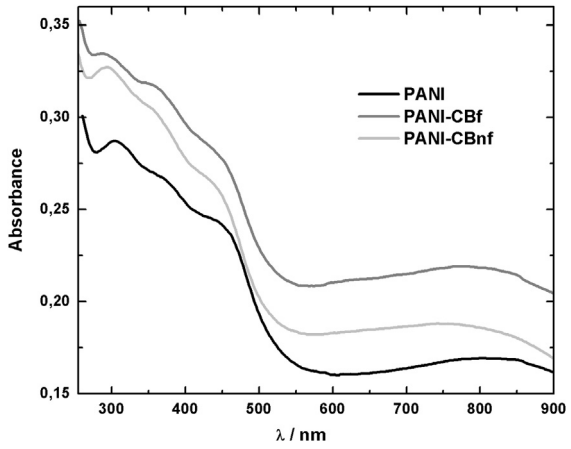

Fig. 5 – UV–Vis spectra of the synthetized nanostructures.

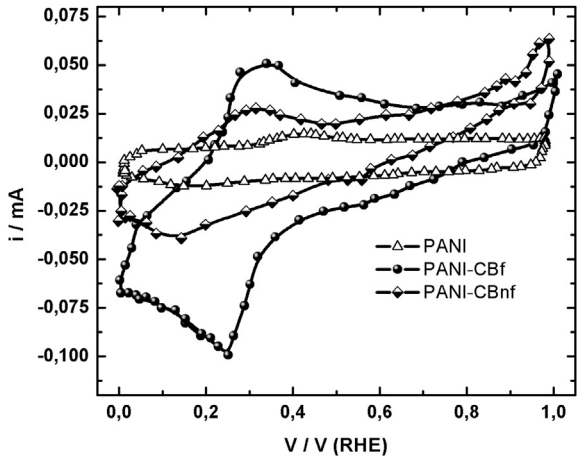

Fig. 6 – Cyclic voltammograms of the nanostructured composite electrodes at 20 mV s^{-1} in 0.5 M H_2SO_4.

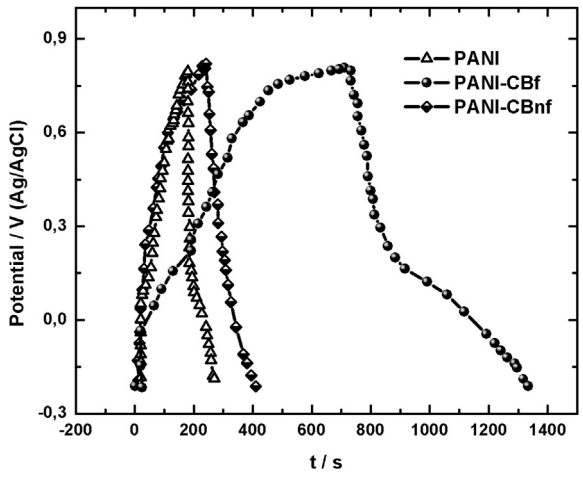

Fig. 7 – Galvanostatic charge–discharge curves of the nanostructured composite electrodes for a current density of 2 A g^{-1} in 0.5 M H_2SO_4.

capacitive behavior in comparison to PANI electrode. This fact may be due to the combined contributions from both PANI and CB structures. However, it can be observed a resistive behavior due mainly to internal resistance.

3.7. *Galvanostatic charge/discharge experiments*

Galvanostatic charge/discharge measurements at different current densities are performed in order to understand the behavior of PANI, PANI-CBf and PANI-CBnf nanostructures for supercapacitor applications. Typical potential versus time profiles for a constant current density of 2 A g^{-1} are shown in Fig. 7. Other supercapacitor materials such as activated carbon, metal oxides, carbon nanotubes and carbon blacks exhibit the observed behavior that corresponds to the ideally triangular shaped charging/discharging pattern [10,28,29]. In the present case, the curves are not straight lines indicating the occurrence of a faradaic reaction among the electrode materials. In addition, an initial potential drop caused by internal resistance can be observed [27].

The electrical parameters of the capacitor, namely, specific capacitance (C_m), specific energy (E_s) and specific power (P_s) are calculated using Eqs. (1)–(3).

$$C_m = \frac{C}{m} = \frac{I\Delta t}{\Delta V m} \quad (1)$$

$$E_s = \frac{I\Delta V \Delta t}{m} \quad (2)$$

$$P_s = \frac{I\Delta V}{m} \quad (3)$$

where C_m is the specific capacitance, I is the charge/discharge current, Δt is the discharge time, ΔV is the potential range and m is the mass of active material [6,27,30].

The formation of PANI and PANI-CBs structures is attained using the self-organization chemical method where the total mass and volume are included in the charge storage. The values of specific capacitance, SC, measured at different current densities are presented in Table 1. Notably high capacitance values of ca. 1490 F g^{-1}, 370 F g^{-1} and 310 F g^{-1} were obtained for PANI-CBf, PANI-CBnf and PANI nanostructures, respectively. PANI-CBf nanocomposites have specific capacitance values very high even evaluated at 40 A g^{-1} [27,31].

Several factors can be considered as responsible for the performance of the PANI-CBf nanocomposites, among others the presence of charge carriers in these arrays and the functionalization after the chemical treatment of the CB particles. It was reported that the charge carriers can either move along the chains within the polymer structure or jump from chain to chain by hopping [32]. Moreover, ab-initio calculations established that the quinoid structures have great affinity for charges that acquire high mobility due to the delocalized polarons [33]. On the other hand, the incorporated CB particles contribute to the SC values providing faradaic pseudocapacitance generated on the superficial oxygenated groups developed during the acid pretreatment. The porous structures have also an important contribution because they operate through both their internal and external interfaces facilitating the electrolyte access.

The stability of the electrodes was evaluated through charge–discharge cycling tests. The specific discharge capacitances of the different electrode materials as a function of the number of cycles are presented in Fig. 8, from runs conducted for 500 cycles at 2 A g^{-1}. The capacitance of PANI-CBf composites is greater than the values corresponding to PANI

Table 1 – Specific capacitances of the synthetized nanomaterials.

Nanomaterial	PANI	PANI-CBf	PANI-CBnf
I (A g^{-1})		C_m (F g^{-1})	
2	314	1486	370
4	134	552	200
10	72	500	171
20	58	470	120
40	42	200	120

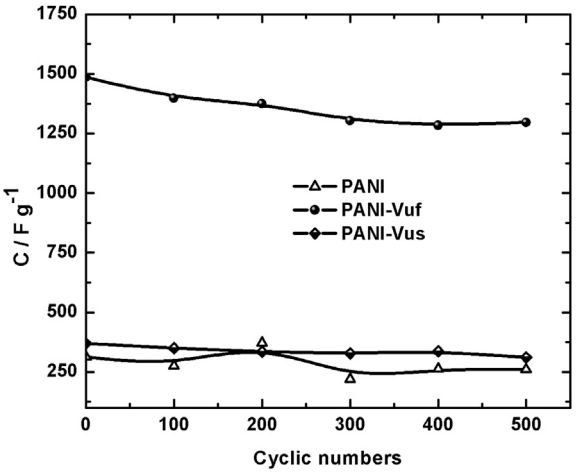

Fig. 8 – Specific capacitance of the nanostructured composite electrodes as a function of the cycle numbers at 2 A g^{-1}.

and PANI-CBnf nanostructures. The loss of capacitance during the charge/discharge cycles is lower than 18% for the three checked materials, being the highest value the corresponding to the PANI nanostructure without additions. These results reveal that the stability of the material can be improved remarkably when introducing CB in the PANI nanostructures.

In Fig. 9, the relationship between the specific power density and specific energy density in the so-called Ragone plot [34] for PANI, PANI-CBf and PANI-CBnf nanostructures is shown. PANI-CBf composites show higher specific power and specific energy values than PANI and PANI-CBnf nanostructures. For PANI-CBf composites, a specific power of 40 kW kg^{-1} and a specific energy of 412 W h kg^{-1} are obtained. It is to point out that for the same specific power value, the specific energy of PANI-CBf composite electrodes is five times larger than the value corresponding to PANI electrodes. Other authors reported SC values of ca. 500 F g^{-1} [16,31].

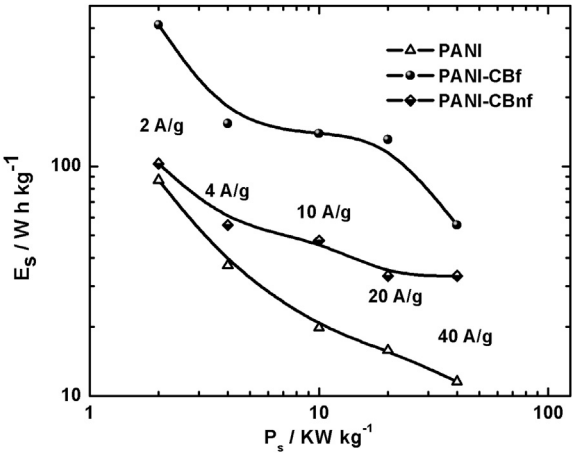

Fig. 9 – Relationship between the specific power density and specific energy density of the nanostructured composite electrodes in 0.5 M H_2SO_4.

For the prepared nanocomposites, the synthetized morphology and the developed porous structure add synergistically to their behavior as possible supercapacitors materials, as both the charge transport and the occurrence of faradaic processes are lightened and a facile access to the electrolyte is provided by the novel structure.

4. Conclusions

Polyaniline nanotubes and PANI-CB nanocomposites were synthetized using a simple method of self-organization. Taking into account their likely application as supercapacitor electrode materials, the electrochemical properties were scrutinized. Firstly, different types of nanostructures were developed during the polymerization process. Nanotubes of polyaniline with an outer diameter of ca. 95 nm and ca.12 μm length were obtained from acid solutions of aniline. When incorporating unfunctionalized or functionalized CB particles, nanobelts and nanotubes were obtained in the former case and nanoparticles, nanobelts, nanotubes and nanosheets when adding CBf.

The formation of the different nanostructures is ascribed to the own chemical polymerization process that provoked a doped PANI state and generated hydrogen links which stabilized the new structures. The electrochemical characterization of the synthetized nanostructures has been carried out applying voltamperommetric and charge/discharge runs.

The developed morphologies influenced the capacitance, specific power and energy values. PANI-CBf nanocomposites displayed improved capacitive properties in H_2SO_4 solutions, namely 1486 F g^{-1} at 2 A g^{-1}. The charge–discharge tests indicated that the loss of capacitance during the charge/discharge cycles was lower than 18% for the synthetized materials and that the introduction of CB particles in the PANI nanostructure improved remarkably their electrochemical behavior.

Acknowledgments

The authors acknowledge the support of SECAT – Facultad de Ingeniería – UNCPBA and CICPBA.

REFERENCES

[1] Winter M, Brodd RJ. What are batteries, fuel cells, and supercapacitors. Chem Rev 2004;104:4245–69.
[2] Pan L, Qiu H, Dou C, Li Y, Pu L, Xu J, et al. Conducting polymer nanostructures: template synthesis and applications in energy storage. Int J Mol Sci 2010;11:2636–57.
[3] Bonnefoi L, Simon P, Fauvarque J, Sarrazin C, Sarrau J, Dugast A. Electrode compositions for carbon power supercapacitors. J Power Sources 1999;80:149–55.
[4] Zhang Y, Feng H, Wu X, Wang L, Zhang A, Xia T, et al. Progress of electrochemical capacitor electrode materials: a review. Int J Hydrogen Energy 2009;34:4889–99.
[5] Yan J, Wei T, Shao B, Ma F, Fan Z, Zhang M, et al. Electrochemical properties of graphene nanosheet/carbon

black composites as electrodes for supercapacitors. Carbon 2010;48:1731–7.
[6] Chen C, Wen TC, Teng H. Polyaniline-deposited porous carbon electrode for supercapacitor. Electrochim Acta 2003;48:641–9.
[7] Toupin M, Bélanger D, Hill IR, Quinn D. Performance of experimental carbon blacks in aqueous supercapacitors. J Power Sources 2005;140:203–10.
[8] Panić VV, Stevanović RM, Jovanović VM, Dekanski AB. Electrochemical and capacitive properties of thin-layer carbon black electrodes. J Power Sources 2008;181:186–92.
[9] Wang ZB, Yin GP, Shao YY, Yang BQ, Shi PF, Feng PX. Electrochemical impedance studies on carbon supported PtRuNi and PtRu anode catalysts in acid medium for direct methanol fuel cell. J Power Sources 2007;165:9–15.
[10] Dong B, He BL, Xu CL, Li HL. Preparation and electrochemical characterization of polyaniline/multi-walled carbon nanotubes composites for supercapacitor. Mat Sci Eng B Solid 2007;143:7–13.
[11] Guang-lei CUI, Xin-hong Z, Lin-jie ZHI, Thomas A, Müllen K. Carbon/nanostructured Ru composites as electrodes for supercapacitors. New Carbon Mater 2007;22:302–6.
[12] Chandrasekhar P. Conducting polymers, fundamentals and applications. A practical approach. Boston-Dordrecht-London: Kluver Academic Publishers; 1999.
[13] Stilwell SM, Park DE. Electrochemistry of conductive polymers: II. Electrochemical studies on growth properties of polyaniline electrochemical science and technology. J Electrochem Soc 1988;135:2254–62.
[14] Aldissi M. Intrinsically conducting polymers: an emerging technology. Burlington-Vermont-USA: N. Division; 1992.
[15] Laslau C, Zujovic Z, Travas-Sejdic J. Theories of polyaniline nanostructure self-assembly: towards an expanded, comprehensive multi-layer theory (MLT). Prog Polym Sci 2010;35:1403–19.
[16] Mu B, Liu P, Wang A. Synthesis of polyaniline/carbon black hybrid hollow microspheres by layer-by-layer assembly used as electrode materials for supercapacitors. Electrochim Acta 2013;88:177–83.
[17] Sivakkumar SR, Kim WJ, Choi JA, MacFarlane DR, Forsyth M, Kim DW. Electrochemical performance of polyaniline nanofibres and polyaniline/multi-walled carbon nanotube composite as an electrode material for aqueous redox supercapacitors. J Power Sources 2007;171:1062–8.
[18] Huang YF, Lin CW. Facile synthesis and morphology control of graphene oxide/polyaniline nanocomposites via in-situ polymerization process. Polymer 2012;53:2574–82.
[19] Bavio MA, Kessler T, Castro Luna AM. Pt–Ru polymeric electrocatalysts used for the determination of carbon monoxide. Thin Solid Films 2013;527:318–22.
[20] Vaccarini L, Goze C, Aznar R, Micholet V, Journet C, Dernier P. Purification procedure of carbon nanotubes. Synth Met 1999;103:2492–3.
[21] Zhou C, Han J, Guo R. Synthesis of polyaniline hierarchical structures in a dilute SDS/HCl solution: nanostructure-covered rectangular tubes. Macromolecules 2009;42:1252–7.
[22] Zujovic ZD, Laslau C, Bowmaker GA, Kilmartin PA, Webber AL, Brown SP, et al. Role of aniline oligomeric nanosheets in the formation of polyaniline nanotubes. Macromolecules 2010;43:662–70.
[23] Boehm HP. Some aspects of the surface chemistry of carbon blacks and other carbons. Carbon 1994;32:759–69.
[24] Reddy KR, Sin BC, Ryu KS, Noh J, Lee Y. In situ self-organization of carbon black–polyaniline composites from nanospheres to nanorods: synthesis, morphology, structure and electrical conductivity. Synth Met 2009;159:1934–9.
[25] Stejskal J, Sapurina I, Trchová M, Konyushenko EN, Holler P. The genesis of polyaniline nanotubes. Polymer 2006;47:8253–62.
[26] Wu KH, Ting TH, Wang GP, Ho WD, Shih CC. Effect of carbon black content on electrical and microwave absorbing properties of polyaniline/carbon black nanocomposites. Polym Degrad Stabil 2008;93:483–8.
[27] Mi H, Zhang X, Yang S, Ye X, Luo J. Polyaniline nanofibers as the electrode material for supercapacitors. Mater Chem Phys 2008;112:127–31.
[28] Pandolfo AG, Hollenkamp AF. Carbon properties and their role in supercapacitors. J Power Sources 2006;157:11–27.
[29] Liu X, Zhang X, Fu S. Preparation of urchinlike NiO nanostructures and their electrochemical capacitive behaviors. Mater Res Bull 2006;41:620–7.
[30] Sumboja A, Wang X, Yan J, See P. Nanoarchitectured current collector for high rate capability of polyaniline based supercapacitor electrode. Electrochim Acta 2012;65:190–5.
[31] Zhou G, Wang D, Li F, Zhang L, Weng Z, Cheng HM. The effect of carbon particle morphology on the electrochemical properties of nanocarbon/polyaniline composites in supercapacitors. New Carbon Mater 2011;26:180–6.
[32] Bredas JL, Street GB. Polarons, bipolarons and solitons in conducting polymer. Acc Chem Res 1985;18:309–15.
[33] Wohlgenannt M, Jiang X, Vardeny Z. Confined and delocalized polarons in π-conjugated oligomers and polymers: a study of the effective conjugation length. Phys Rev B 2004;69:2412041R.
[34] Gupta V, Miura N. Polyaniline/single-wall carbon nanotube (PANI/SWCNT) composites for high performance supercapacitors. Electrochim Acta 2006;52:1721–6.